

Supporting Information for

‘Darker-than-Black’ PbS Quantum Dots:

Enhancing Optical Absorption of Colloidal Semiconductor

Nanocrystals via Short Conjugated Ligands

Carlo Giansante,^{†‡} Ivan Infante,^{◇,°} Eduardo Fabiano,^{†,‡} Roberto Grisorio,[#] Gian
Paolo Suranna,[#] Giuseppe Gigli^{‡,§}*

[†] *Center for Biomolecular Nanotechnologies @UNILE, Istituto Italiano di Tecnologia, via Barsanti 1,
73010 Arnesano (LE), Italy*

[‡] *NNL-CNR Istituto di Nanoscienze, via per Arnesano, 73100 Lecce, Italy*

[◇] *Kimika Fakultatea, Euskal Herriko Unibersitatea and Donostia International Physics Center (DIPC), 20080,
CP1072, San Sebastian, Spain*

[°] *Department of Theoretical Chemistry, Faculty of Sciences, Vrije Universiteit Amsterdam, De Boelelaan 1083,
1081 HV, Amsterdam, The Netherlands*

[#] *DICATECh - Dipartimento di Ingegneria Civile, Ambientale, del Territorio, Edile e di Chimica,
Politecnico di Bari, via Orabona 4, 70125 Bari, Italy*

[§] *Dipartimento di Matematica e Fisica ‘E. De Giorgi’, Università del Salento, via per Arnesano, 73100
Lecce, Italy*

*e-mail: carlo.giansante@iit.it

Materials. All chemicals were of the highest purity available unless otherwise noted and were used as received. Lead oxide (PbO, 99.999%), Cadmium oxide (CdO, 99.5%), oleic acid ($\text{Ol}\cdot\text{H}^+$, technical grade 90%), 1-octadecene (ODE, technical grade 90%), bis(trimethylsilyl)sulfide (TMS, synthesis grade), p-methylbenzenethiol ($\text{ArS}^-\cdot\text{H}^+$, 98%), p-aminothiophenol ($\text{D-ArS}^-\cdot\text{H}^+$, 97%), p-(trifluoromethyl)thiophenol ($\text{A-ArS}^-\cdot\text{H}^+$, 97%), p-toluic acid ($\text{ArCO}_2^-\cdot\text{H}^+$, 98%), p-toluidin (ArNH_2 , 99%), 1-butanethiol (AlSH, 99%), were purchased from Sigma-Aldrich. Tri-n-octylphosphine oxide (TOPO 99%), tri-n-octylphosphine (TOP, 97%), Sulfur (99%), and Selenium (Se, 99,99%) were purchased from Strem Chemicals. Octadecylphosphonic acid (ODPA, 99%) and hexylphosphonic acid (HPA, 99%) were purchased from Polycarbon Industries. Triethylamine (Et_3N , $\geq 99.5\%$) was purchased from Fluka. All solvents were anhydrous and were used as received. Acetone (Ac, 99.8%) was purchased from Merck. Acetonitrile (ACN, 99.8%), chloroform (CHCl_3 , 99.8%), dichloromethane (DCM, 99.8%), o-dichlorobenzene (DCB, 99%), hexane (Hex, 95%), methanol (MeOH, 99.8%), tetrachloroethylene (TCE, 99%), and toluene (Tol, 99.8%) were purchased from Sigma-Aldrich.

Colloidal QD synthesis:

All QDs were synthesized in a three-neck flask connected to a standard Schlenk line setup under oxygen- and water-free conditions.

Synthesis of PbS/OI QDs:

In a typical synthesis,¹ 2 mmol of PbO (450 mg) and 4 mmol (1140 mg) of oleic acid were mixed in 10 g of ODE. The mixture was vigorously stirred and deaerated through repeated cycles of vacuum application and purging with nitrogen at about 80 °C. Then, the mixture was heated to above 100 °C to allow dissolution of PbO until the solution became colorless and optically clear, indicating the formation of lead(II)-oleate complex. The solution was cooled at 80 °C and repeatedly subjected to vacuum in order to remove water formed upon lead(II)-oleate complex formation. The solution was then heated again under nitrogen flow and stabilized at 110°C. At this point 1 mmol of TMS (210 μL) in 2 mL of TOP was swiftly injected. The heating mantle was immediately removed and the resulting black colloidal solution was allowed to naturally cool to room temperature. After the synthesis, PbS/OI QDs were

transferred to a nitrogen-protected glove box. The QDs were precipitated using excess Ac, centrifuged at 4000 rpm for 7 min and then redissolved in Tol. Centrifugation at 4000 rpm for 5 minutes and filtration through a 0.2 μm polytetrafluoroethylene (PTFE) membrane were carried out to discard insoluble products and possible agglomerates. Additional precipitation-redissolution cycles were applied to remove any excess unbound surfactants. A 1 mM QD solution was prepared and stored at room temperature in a glove box for subsequent use. The concentration and diameter of the resulting PbS/OI QDs were estimated spectrophotometrically from known absorption coefficient values.² The PbS/OI QD size was varied around 3 nm by changing the amount of oleic acid added to PbO.

Synthesis of CdS/OI QDs:

In a typical synthesis,³ 1 mmol of CdO (128 mg) was mixed with 3 mmol (850 mg) of oleic acid and 50 g of ODE. The mixture was vigorously stirred and deaerated through repeated cycles of vacuum application and purging with nitrogen at about 80 °C. Then, the mixture was heated to above 200 °C to allow dissolution of CdO until the solution became colorless and optically clear, indicating the formation of cadmium(II)-oleate complex. The solution was cooled at 80 °C and repeatedly subjected to vacuum in order to remove water formed upon cadmium(II)-oleate complex formation. The solution was then heated again under nitrogen flow and stabilized at 300°C. At this point 0.5 mmol of S precursor (0.016g of S in 10g of ODE, previously prepared under nitrogen atmosphere) was swiftly injected and CdS QDs were allowed to grow at 250 °C for about 10 minutes. The heating mantle was then removed and the reaction quenched by compressed air. After the synthesis, CdS/OI QDs were transferred to a nitrogen-protected glove box. The QDs were repeatedly precipitated using excess Ac and then redissolved in Tol, filtered through a 0.2 μm polytetrafluoroethylene (PTFE) membrane then stored at room temperature in a glove box for subsequent use as 1 mM solutions. The concentration and diameter of the resulting CdS/OI QDs were estimated spectrophotometrically from known absorption coefficient values.⁴

Synthesis of CdS QDs capped with phosphine oxide/phosphonic acid ligands:

In a typical procedure,⁵ TOPO (3.300g), ODPA (0.600g) and CdO (0.100g) were mixed in a three-neck flask, heated to ca. 90°C and repeatedly subjected to vacuum-nitrogen cycles. Under nitrogen atmosphere, the reaction mixture was then heated to above 300°C to dissolve the CdO until the solution turns optically clear and colorless. The heating mantle was removed to cool the flask to about 90 °C and again subjected to vacuum-nitrogen cycles.

The temperature was then raised to 320°C and let stabilize then a mixture of TMS (0.170g) and TBP (3g) was injected swiftly. The heat-controller was set to 250°C and the nanocrystals were allowed to grow at this temperature to adjust their final diameter. Then the reaction was quenched by compressed air. Afterwards, the nanocrystals were precipitated with MeOH, they washed by repeated re-dissolution in Tol and precipitation with the addition of MeOH, and finally kept in Tol. The concentration and diameter of the resulting CdS QDs were estimated spectrophotometrically from known absorption coefficient values.⁴

Synthesis of CdSe QDs capped with phosphine oxide/phosphonic acid ligands:

In a typical procedure,⁵ TOPO (3.000g), ODPA (0.280g) and CdO (0.060g) were mixed in a three-neck flask, heated to ca. 90°C and repeatedly subjected to vacuum-nitrogen cycles. Under nitrogen atmosphere, the reaction mixture was then heated to above 300°C to dissolve the CdO until the solution turns optically clear and colorless. The heating mantle was removed to cool the flask to about 90 °C and again subjected to vacuum-nitrogen cycles. The temperature was then raised to the required injection temperature (around 380 °C) and let stabilize. Then swift injection of the Se:TOP solution (0.058g Se + 0.360g TOP) followed . The injection temperature and the reaction time were modified in order to synthesize CdSe dots of different sizes. The reaction was then quenched by compressed air. Afterwards, the nanocrystals were precipitated with MeOH, washed by repeated re-dissolution in Tol and precipitation with the addition of MeOH, and finally kept in Tol or TOP for use in the synthesis of core/shell QDs. The concentration and diameter of the resulting CdSe QDs were estimated spectrophotometrically from known absorption coefficient values.⁴

Synthesis of CdSe/CdS core/shell QDs:

In a typical synthesis of CdSe/CdS core/shell nanorods,⁵ CdO (0.090g) is mixed in a flask together with TOPO (3g), ODPA (0.290g), and HPA (0.080g). After repeatedly pumping the flask to vacuum for about 1 hour at 90°C, the resulting solution is heated above 300°C to dissolve the CdO until the solution turns optically clear and colorless. The heating mantle was removed to cool the flask to about 90 °C and again subjected to vacuum-nitrogen cycles. The temperature was then raised to the required injection temperature (around 350 °C) and let stabilize. The S-precursor/ CdSe QD-seed solution is prepared by dissolving S in TOP (0.120g S + 1.5g TOP) and adding to this 200 µl of a 400µM solution of CdSe QDs in TOP. Such a solution was quickly injected in the flask. The nanocrystals

were allowed to grow for about 6-8 minutes after the injection, after which the heating mantle was removed and the reaction quenched by compressed air. Afterwards, the nanorods were precipitated with MeOH, washed by repeated re-dissolution in Tol and precipitation with the addition of MeOH, and finally kept in Tol.

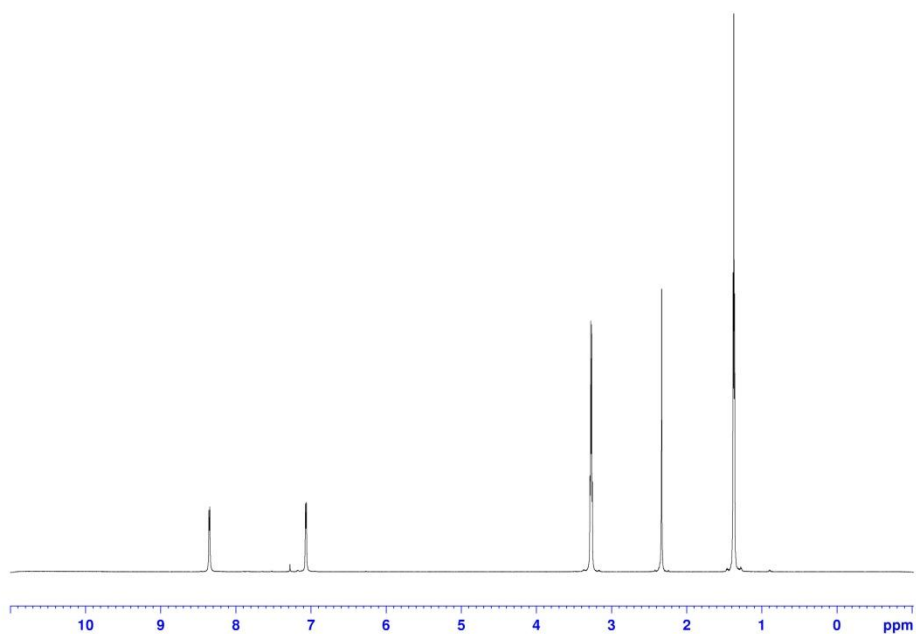


Figure S1. ^1H -NMR spectrum of $\text{ArCS}_2^-/\text{Et}_3\text{NH}^+$ ligand.

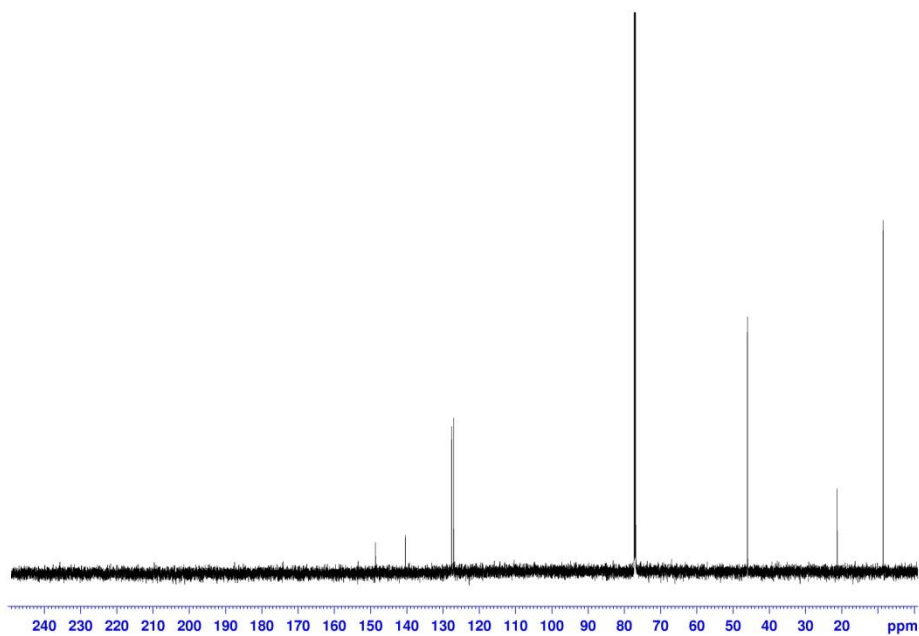


Figure S2. ^{13}C -NMR spectrum of $\text{ArCS}_2^-/\text{Et}_3\text{NH}^+$ ligand.

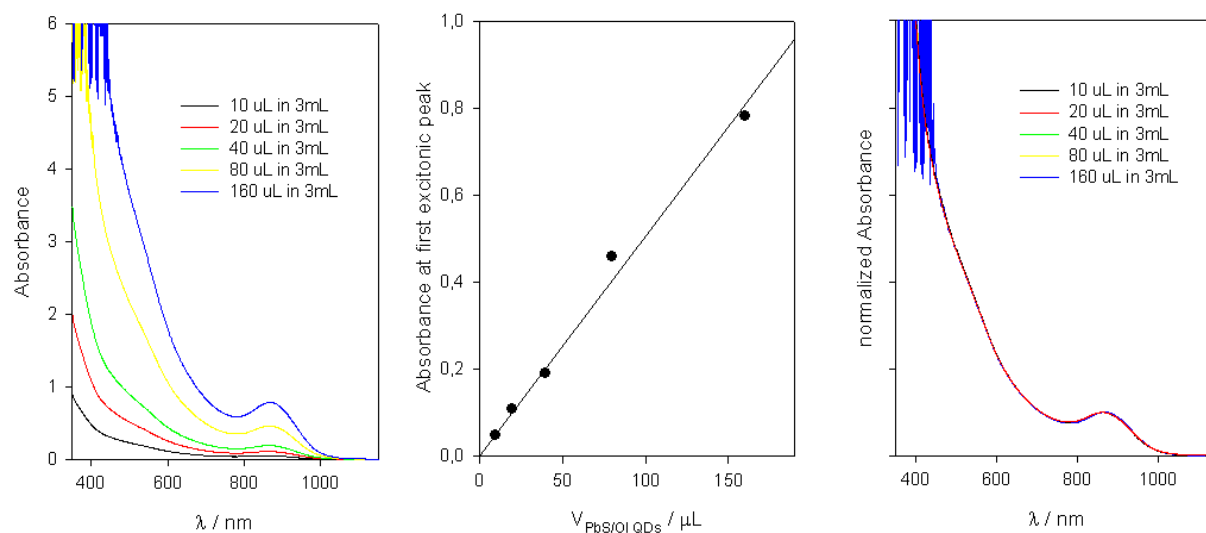


Figure S3. Optical absorption spectra of as-synthesized PbS/OI QDs obtained upon addition of increasing aliquots from a PbS/OI QD stock solution to 3 mL of dichloromethane (as reported in the legends). Left panel) as-recorded absorption spectra; central panel) plot of the Absorbance at first excitonic peak and linear regression ($\chi^2 = 0.985$); right panel) normalized absorption spectra as in the left panel.

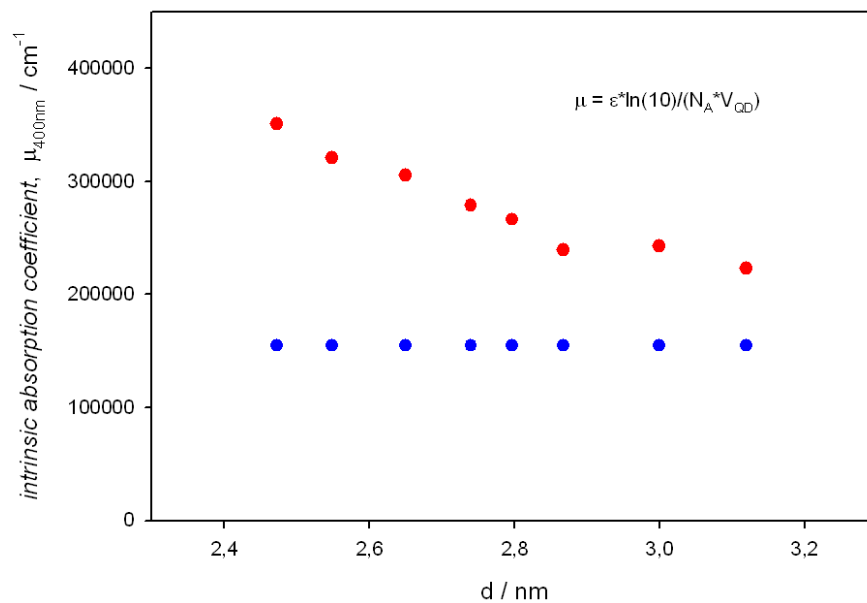


Figure S4. Intrinsic absorption coefficient, μ , at 400 nm of as-synthesized PbS/OI QDs (blue circles) estimated according to calculations derived from effective medium theory.² Intrinsic absorption coefficient at 400 nm of PbS/ArS QDs (red circles) estimated by using Lambert-Beer law for titration experiments in a closed system.

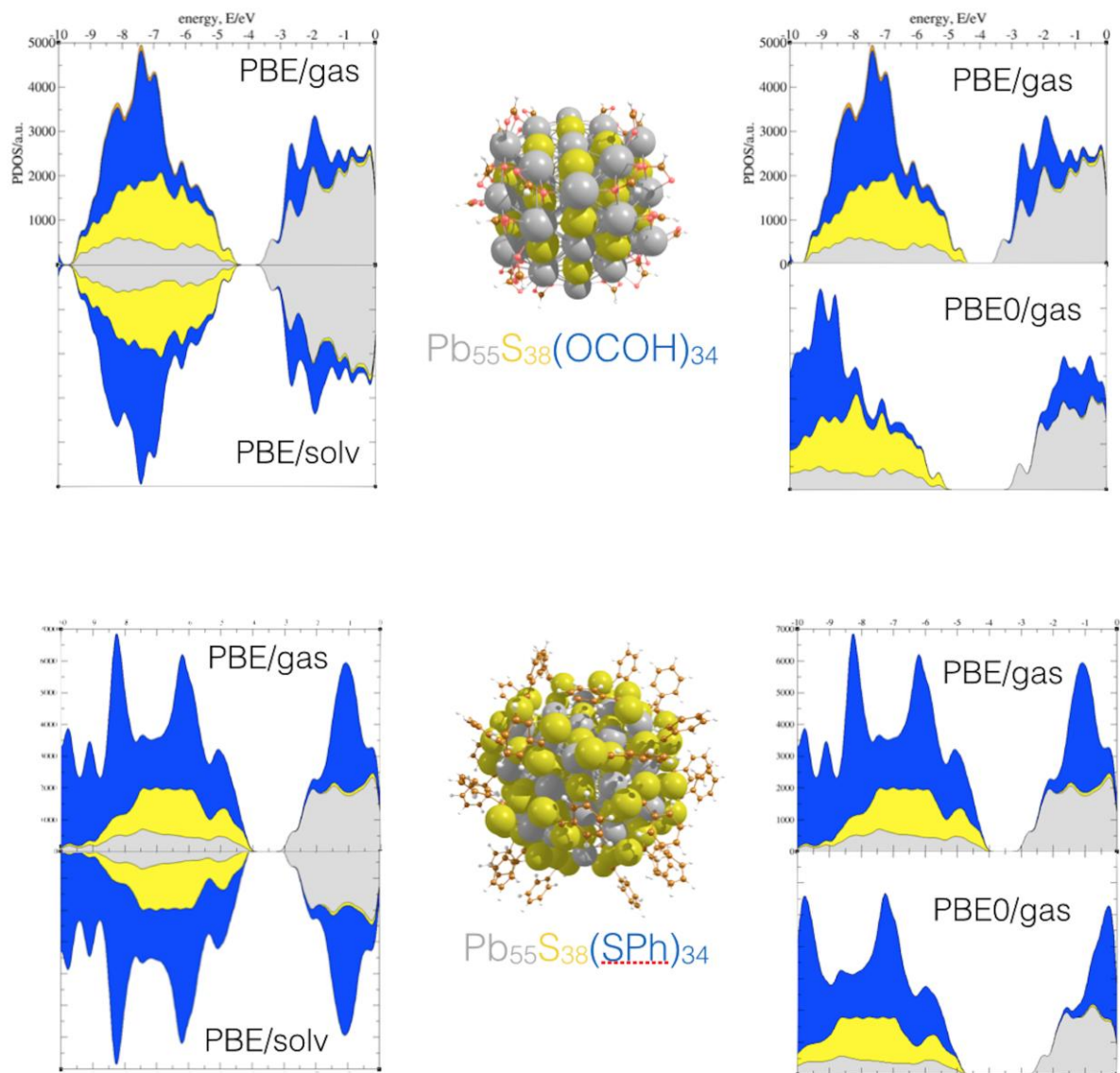


Figure S5. PDOS for the model $(\text{Pb}_{55}\text{S}_{38})^{34+}$ clusters capped with 34 formiate ligands (top panel) and 34 benzenethiolate ligands (bottom panel); Pb orbitals of the inorganic cluster are shown in grey, S orbitals of the inorganic cluster in yellow, orbitals of the ligands in blue. Left panels show the negligible solvation effect (considering dichloromethane as surrounding medium) on the calculated PDOS using PBE functional for both ligand/cluster models. Right panels show the qualitative independence of our results from the employed level of theory (PBE and PBE0 functional in the gas-phase) clearly showing the relevant contribution of the conjugated thiolate ligands' orbitals to the calculated PDOS.

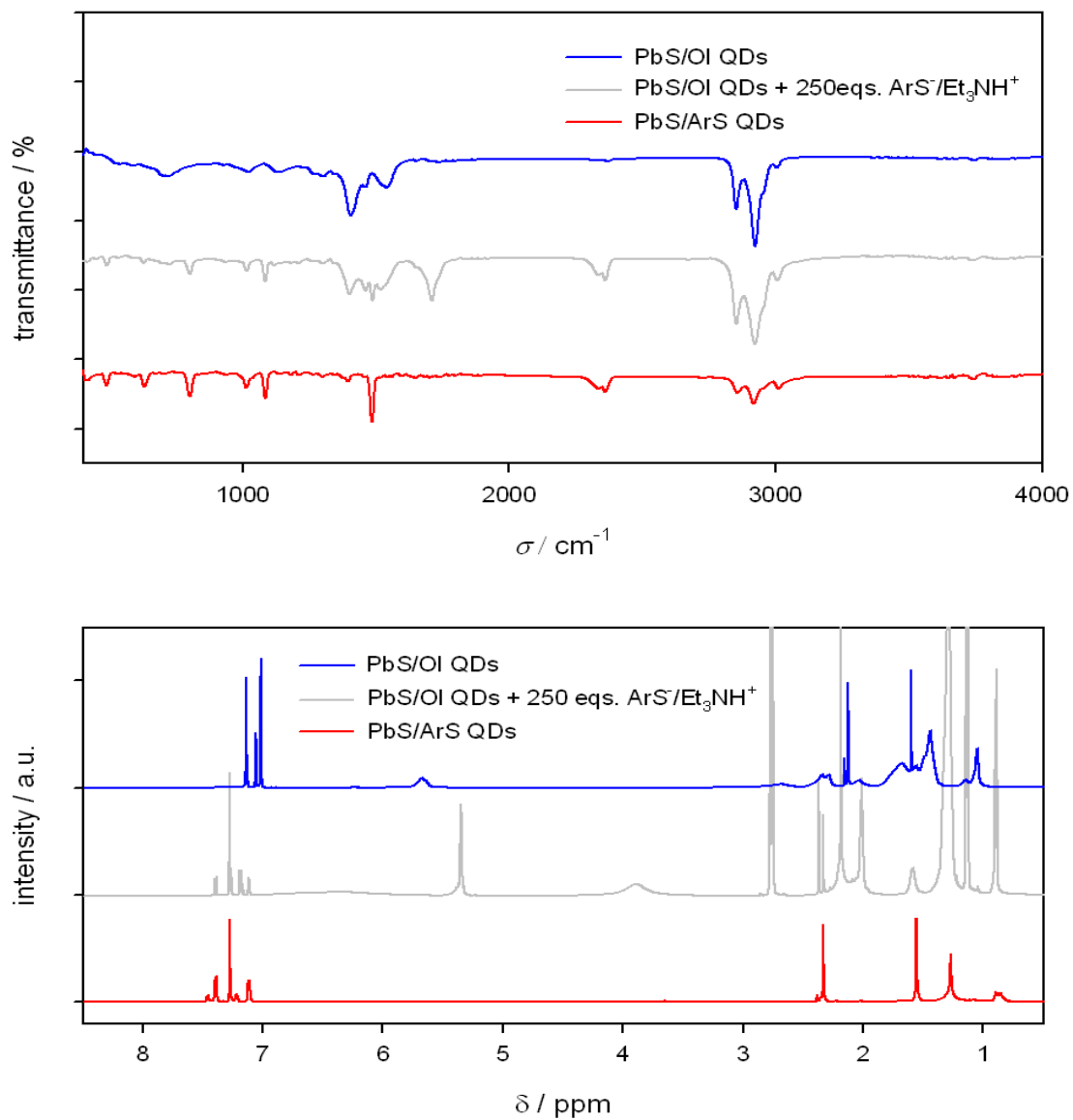


Figure S6. Top panel) FTIR spectra of solids of PbS/OI QDs (blue line), PbS/OI QDs upon addition of 250 equivalents of $\text{ArS}^-/\text{Et}_3\text{NH}^+$ (grey line), and purified PbS/ArS QDs (red line). Spectra have been vertically offset for clarity. Bottom panel) $^1\text{H-NMR}$ spectra of 0.1 mM solutions of PbS/OI QDs (in $\text{C}_6\text{D}_5\text{CD}_3$, blue line), PbS/OI QDs upon addition of 250 equivalents of $\text{ArS}^-/\text{Et}_3\text{NH}^+$ (in CDCl_3 , grey line), and purified PbS/ArS QDs (in CDCl_3 , red line). Spectra have been vertically offset for clarity.

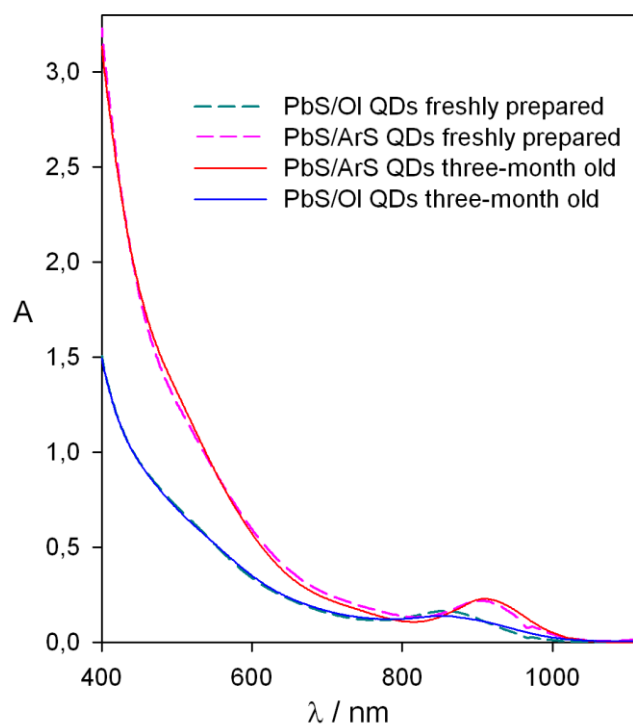


Figure S7. Optical absorption spectra of freshly prepared (dashed lines) and three-month old (solid lines) PbS/OI QDs (tones of blue) and PbS/ArS QDs (tones of red) in dichloromethane solution.

Calculation of surface binding sites on the PbS QDs:⁷

The number of atoms, N_{tot} , in a sphere of diameter d is:

$$N_{tot} = \frac{4\pi}{3} \left(\frac{d}{a} \right)^3 \quad (1)$$

where a is the PbS lattice constant, $a = 0.5936$ nm.

The maximum number of surface atoms, N_{surf}^{max} , can be thus calculated:

$$N_{surf}^{max} = \frac{4\pi}{3} \left[\left(\frac{d}{a} \right)^3 - \left(\frac{d-a}{a} \right)^3 \right] \quad (2)$$

Assuming a stoichiometric PbS core surrounded by a Pb shell,⁸ the ratio between Pb and S atoms is:

$$\left(\frac{Pb}{S} \right)_{tot} = \frac{N_{tot} + N_{surf}}{N_{tot} - N_{surf}} \quad (3)$$

A PbS QD with a diameter of 2.8 nm is constituted by 440 atoms, with a maximum of 225 atoms on its surface. Considering the $(Pb/S)_{tot} = 1.8$, as calculated by ICP-AES, the Pb atoms on the surface are 126. The number of added ligands divided by the number of excess surface Pb atoms per PbS/OI QD yields two thiolate-terminated ligands per each surface Pb atom, as plotted in Figure 4f.

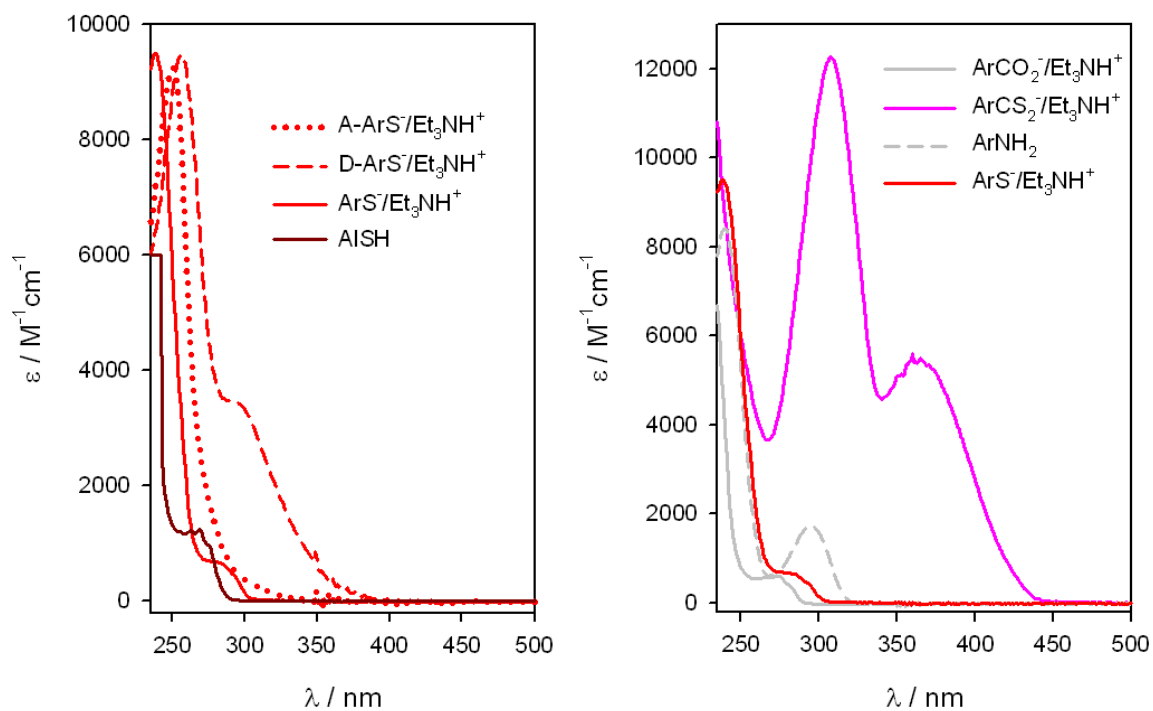


Figure S8. Optical absorption spectra of the ligands employed in this work in air-equilibrated dichloromethane solutions.

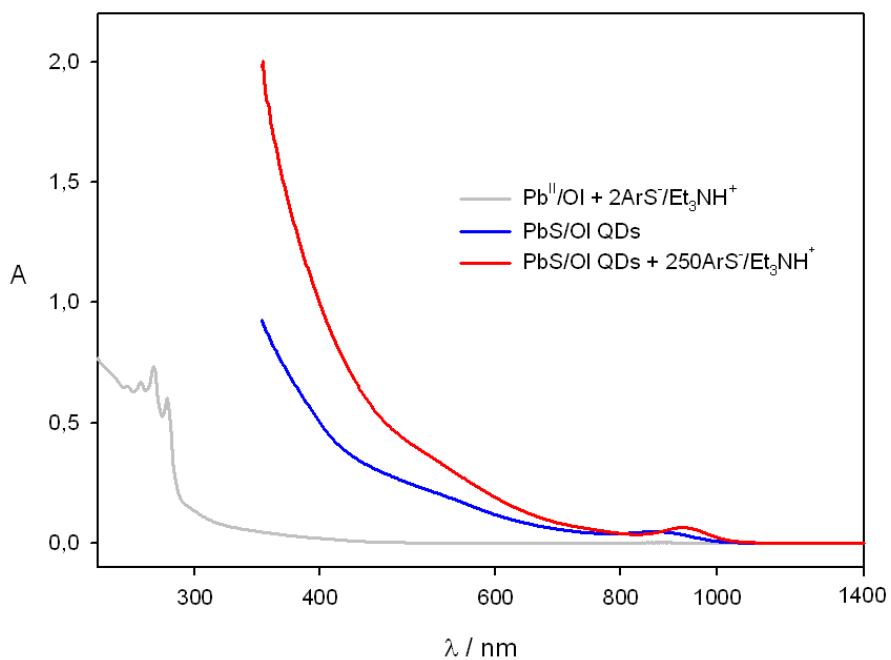


Figure S9. Optical absorption spectrum of Pb(II)/OI upon addition of two equivalents of $\text{ArS}^-/\text{Et}_3\text{NH}^+$ (grey line) and comparison with PbS/OI QDs (blue line) upon addition of two equivalents of $\text{ArS}^-/\text{Et}_3\text{NH}^+$ per excess Pb atom (red line).

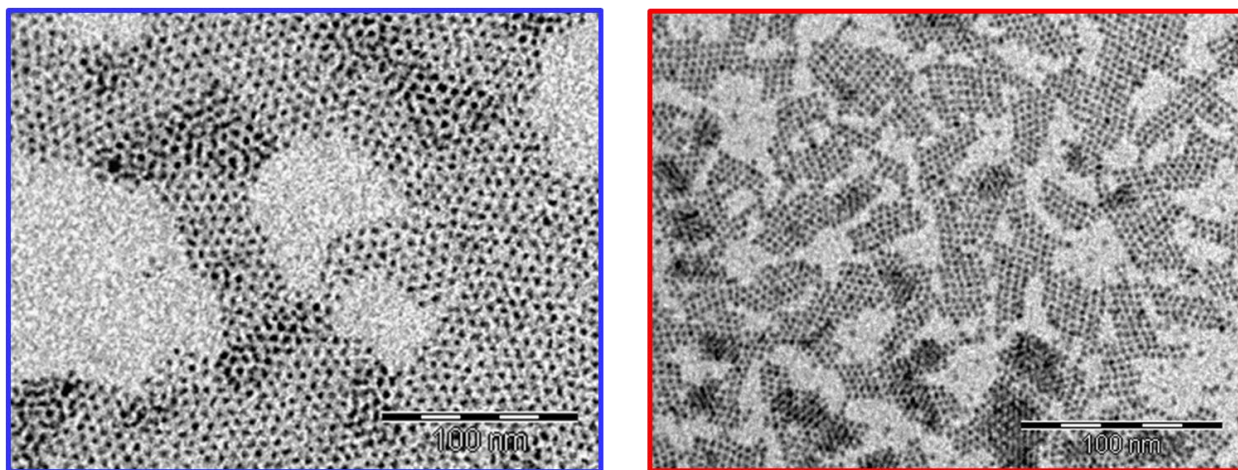


Figure S10. TEM images of as-synthesized PbS/OI QDs (left panel) and of purified PbS/ArS QDs (right panel).

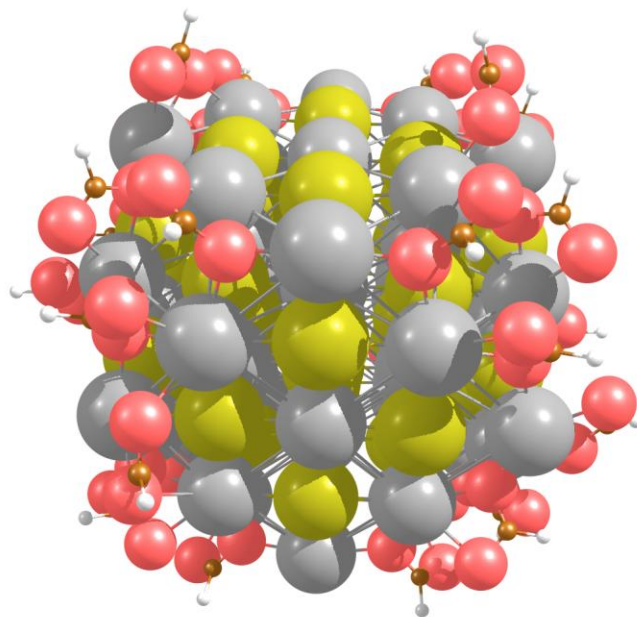


Figure S11. $[(\text{Pb}_{55}\text{S}_{38})^{34+}] \cdot 34(\text{Fo}^-)$ cluster model for PbS/OI QD. Fo^- stands for formiate.

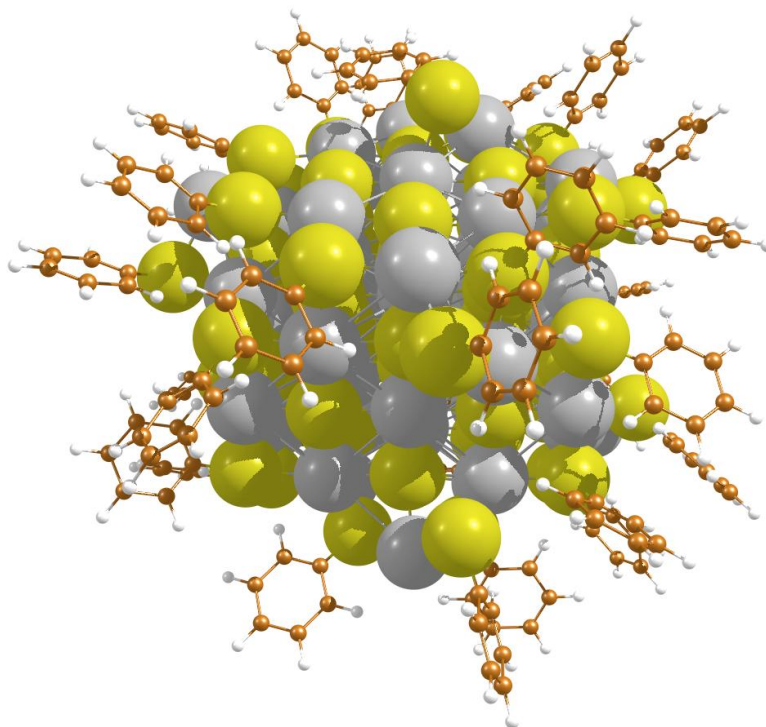


Figure S12. $[(\text{Pb}_{55}\text{S}_{38})^{34+}] \cdot 34(\text{PhS}^-)$ cluster model for PbS/ArS QD. PhS^- stands for benzenethiolate.

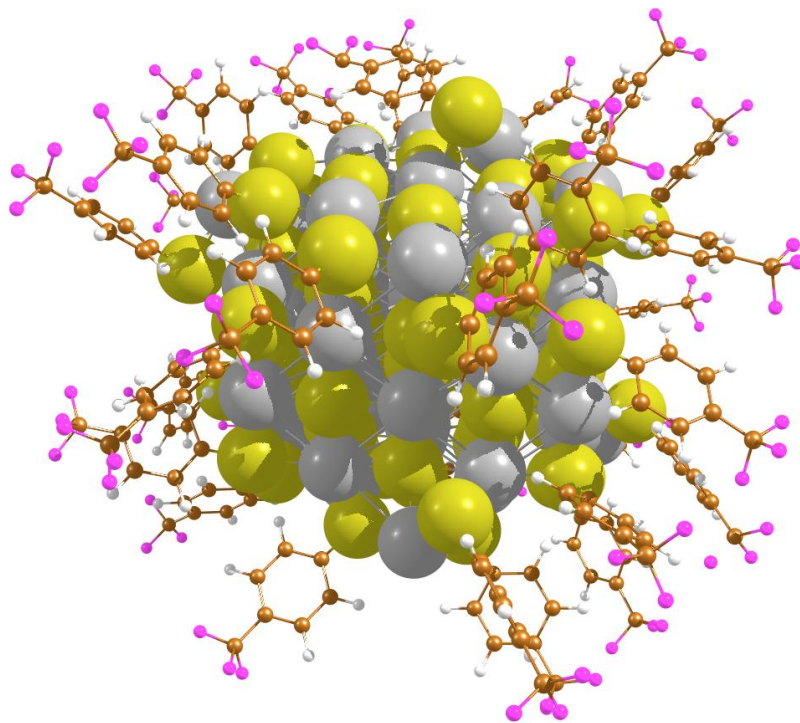


Figure S13. $[(\text{Pb}_{55}\text{S}_{38})^{34+}] \cdot 34(\text{A-ArS}^-)$ cluster model for PbS/A-ArS QD.

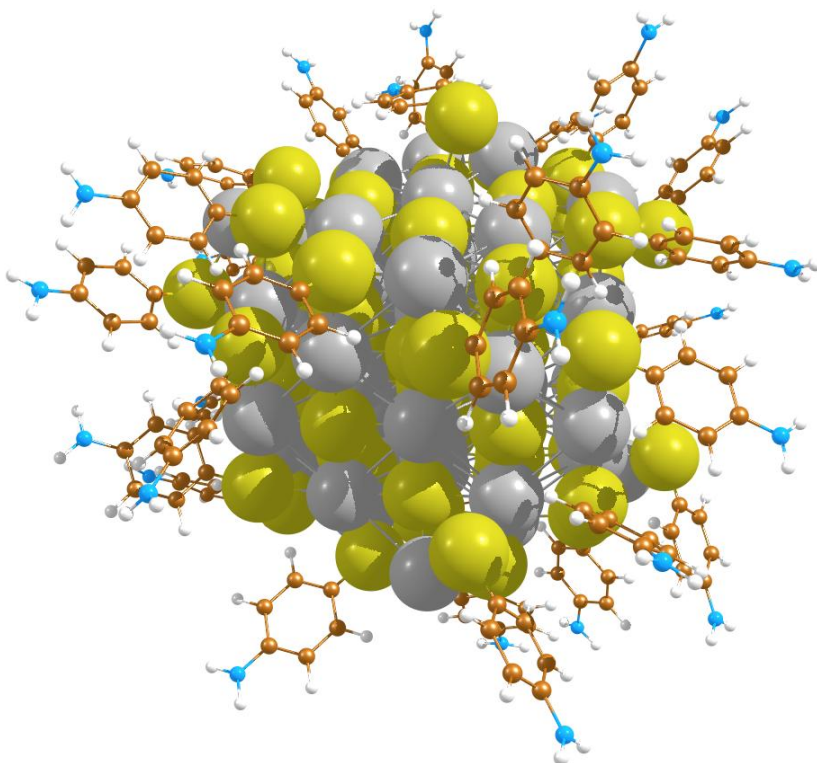


Figure S14. $[(\text{Pb}_{55}\text{S}_{38})^{34+}] \cdot 34(\text{D-ArS}^-)$ cluster model for PbS/D-ArS QD.

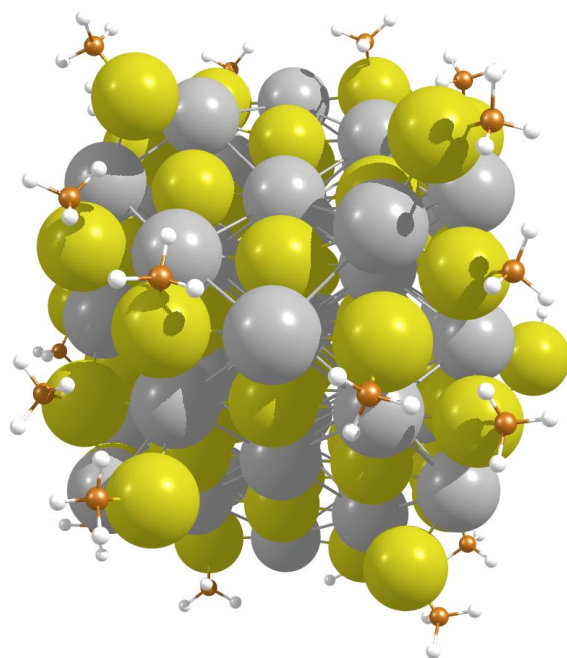


Figure S15. $[(\text{Pb}_{55}\text{S}_{38})^{34+}] \cdot 34(\text{MeS}^-)$ cluster model for PbS/AIS QD. MeS^- stands for methylthiolate.

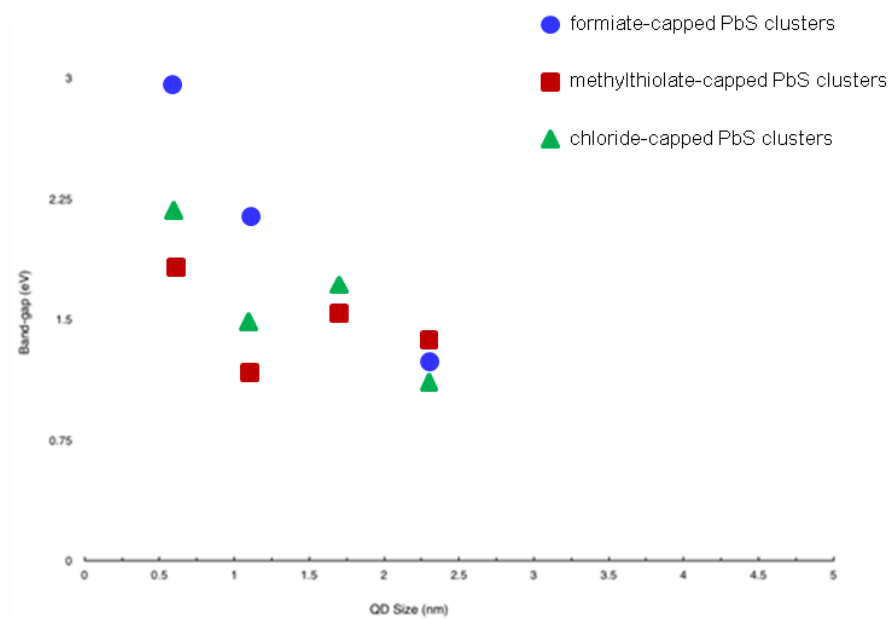


Figure S16. Cluster-size dependence of model clusters $-(\text{Pb}_6\text{S})^{10+}$, $(\text{Pb}_{19}\text{S}_6)^{26+}$, $(\text{Pb}_{44}\text{S}_{19})^{50+}$, and $\text{Pb}(\text{Pb}_{55}\text{S}_{38})^{34+}$ capped with anionic ligands, which guarantee charge neutrality.

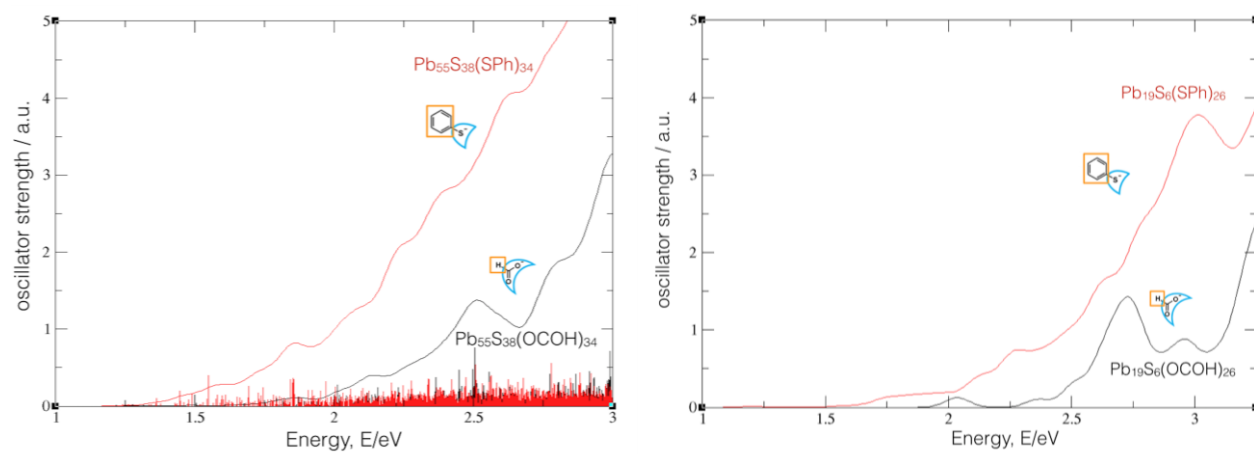


Figure S17. Calculated TDDFT transitions (vertical lines in left panel) and spectra for ligand/clusters based on $(\text{Pb}_{55}\text{S}_{38})^{34+}$ (left panel) and $(\text{Pb}_{19}\text{S}_6)^{26+}$ (right panel) clusters capped with benzenethiolate ligands (red spectra) and formiate ligands (black spectra) guaranteeing charge neutrality.

Effective Medium Theory Calculations:

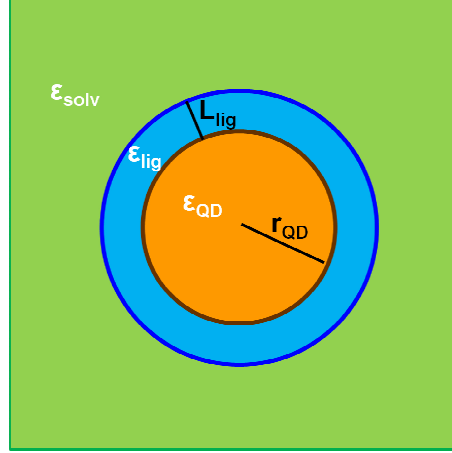


Figure S18. Schematic representation of our inorganic core/ ligand shell/ solvent medium system, highlighting the parameter used below to describe the polarization effect induced by the replacing ligand shell on the local field factor and the first excitonic peak energy.

The observed increase of energy-integrated molar absorption coefficient, $\alpha_{gap}/\alpha_{gap}^0$ (the superscript 0 is referred to as-synthesized PbS/OI QDs), can be thus related to a local enhancement of the electric field induced by the ligand shell and expressed as:^{9,10}

$$\frac{\alpha_{gap}}{\alpha_{gap}^0} = \frac{f_{gap} |f_{LF}|^2}{f_{gap}^0 |f_{LF}^0|^2} \quad (4)$$

where f_{gap} is the QD oscillator strength at the optical bandgap and f_{LF} is the local electric field factor according to the following expression:

$$|f_{LF}|^2 = \left| \frac{9\epsilon_{lig}\epsilon_{solv}}{a\epsilon_{lig} + 2b\epsilon_{solv}} \right|^2 \quad (5)$$

with,

$$a = \epsilon_{QD} \left(3 - 2 \frac{(L_{lig} + r_{QD})^3 - r_{QD}^3}{(L_{lig} + r_{QD})^3} \right) + 2\epsilon_{lig} \frac{(L_{lig} + r_{QD})^3 - r_{QD}^3}{(L_{lig} + r_{QD})^3} \quad (6)$$

$$b = \epsilon_{QD} \frac{(L_{lig} + r_{QD})^3 - r_{QD}^3}{(L_{lig} + r_{QD})^3} + \epsilon_{lig} \left(3 - \frac{(L_{lig} + r_{QD})^3 - r_{QD}^3}{(L_{lig} + r_{QD})^3} \right) \quad (7)$$

Assuming high-frequency dielectric constant values as $\epsilon_{\text{QD}} = 17.2$ for PbS¹¹ and $\epsilon_{\text{solv}} = 1.98$ for dichloromethane,¹² whereas ϵ_{lig} is estimated as 2.13 for oleic acid and 2.52 for p-methylbenzenethiol (calculated as the square of the refractive index),¹³ whereas the ligand length, L_{lig} , is assumed as 1.8 nm for oleic acid and 0.6 nm for p-methylbenzenethiol, the calculated ligand-induced polarization effect on the local field factor is negligible (see plot

of $\frac{|f_{LF}^0|^2}{|f_{LF}|^2}$ as a function of QD radius, r_{QD}), thus accounting for an effective increase of the QD oscillator

strength induced by arenethiolate ligands.

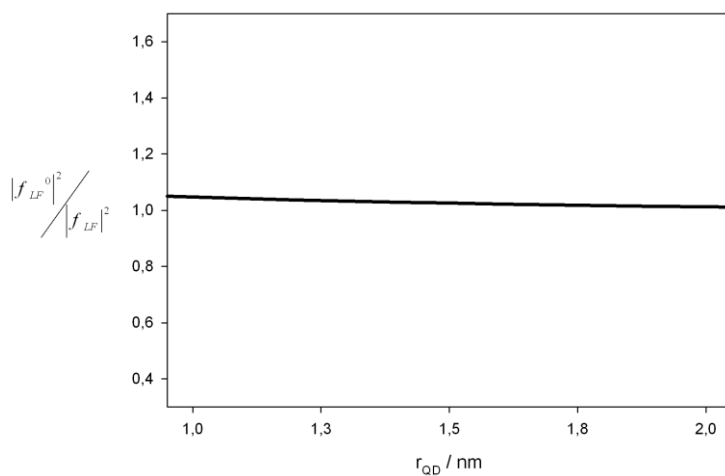


Figure S19. Plot of $\frac{|f_{LF}^0|^2}{|f_{LF}|^2}$ as a function of QD radius, r_{QD} , calculated as discussed above.

Analogously, the polarization effect on the energy of the first exciton transition can be described under the assumption that bulk transport gap, kinetic energies of the electron and the hole due to quantum confinement, and their Coulomb attraction are related only to the QD, thus the observed bathochromic shift, ΔE_{gap} , can be derived according to:^{14,15}

$$\Delta E_{\text{gap}} = \delta^0 - \delta \quad (8)$$

with,

$$\delta = \frac{\pi e^2}{2\epsilon_{\text{QD}}\epsilon_0 r_{\text{QD}}} \sum_{l=1}^{\infty} r_{\text{QD}}^{2l+1} A_l \int_0^1 [j_0(\pi x)]^2 x^{2l+2} dx \quad (9)$$

where ϵ_0 and e are the vacuum permittivity and fundamental charge for the electron, respectively, $j_0(x) = \sin(x)/x$ is the zero-order spherical Bessel function, and the term A_l is given by,

$$A_l = \frac{l+1}{r_{\text{QD}}^{2l+1}} \frac{r_{\text{QD}}^{2l+1} (\epsilon_{\text{lig}} - \epsilon_{\text{solv}}) [\epsilon_{\text{QD}} + l(\epsilon_{\text{QD}} + \epsilon_{\text{lig}})] + (r_{\text{QD}} + L_{\text{lig}})^{2l+1} (\epsilon_{\text{QD}} - \epsilon_{\text{lig}}) [\epsilon_{\text{solv}} + l(\epsilon_{\text{lig}} + \epsilon_{\text{solv}})]}{r_{\text{QD}}^{2l+1} (\epsilon_{\text{QD}} - \epsilon_{\text{lig}}) [\epsilon_{\text{lig}} - \epsilon_{\text{solv}}] l(l+1) + (r_{\text{QD}} + L_{\text{lig}})^{2l+1} [\epsilon_{\text{lig}} + l(\epsilon_{\text{QD}} + \epsilon_{\text{lig}})] [\epsilon_{\text{solv}} + l(\epsilon_{\text{lig}} + \epsilon_{\text{solv}})]} \quad (10)$$

which accounts for an infinite potential well outside the QD.

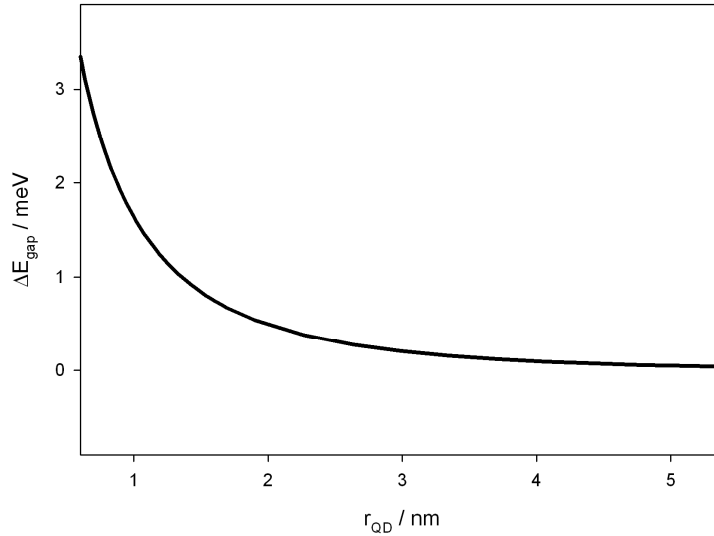


Figure S20. Plot of ΔE_{gap} as a function of QD radius, r_{QD} , calculated as discussed above.

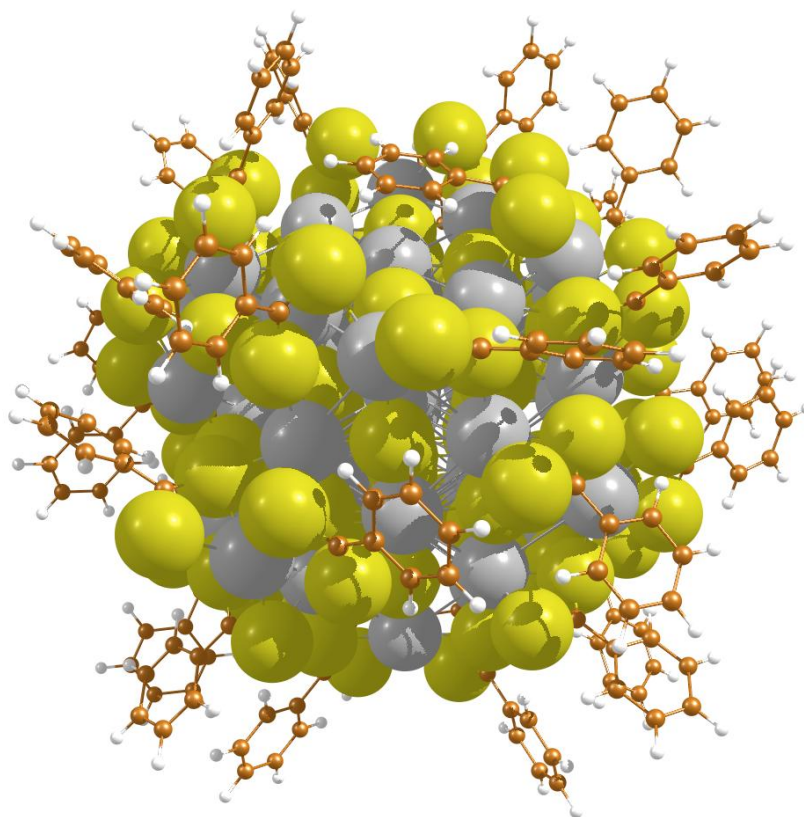


Figure S21. $[(\text{Pb}_{55}\text{S}_{38})^{34+}] \cdot 34(\text{PhCS}_2^-)$ cluster model for PbS/ArCS₂ QD.

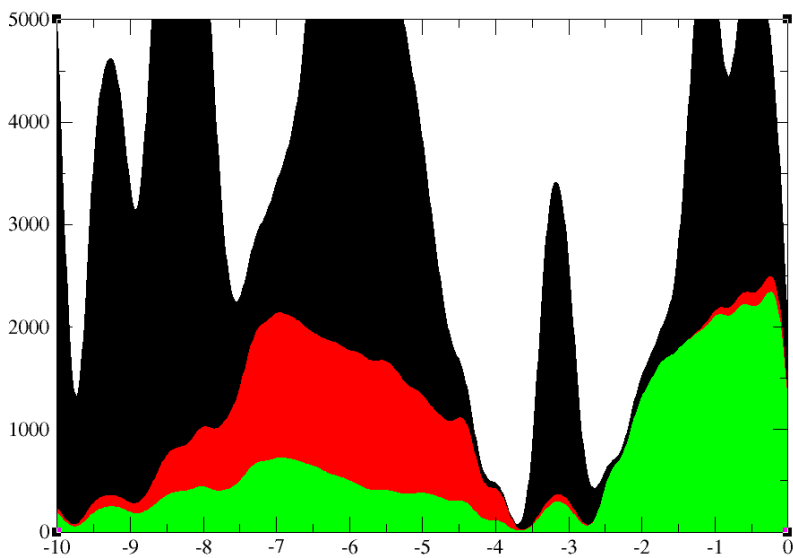


Figure S22. PDOS of $[(\text{Pb}_{55}\text{S}_{38})^{34+}] \cdot 34(\text{PhCS}_2^-)$ model. Pb orbitals of the inorganic cluster are shown in green, S orbitals of the inorganic cluster in red, orbitals of the ligand in black.

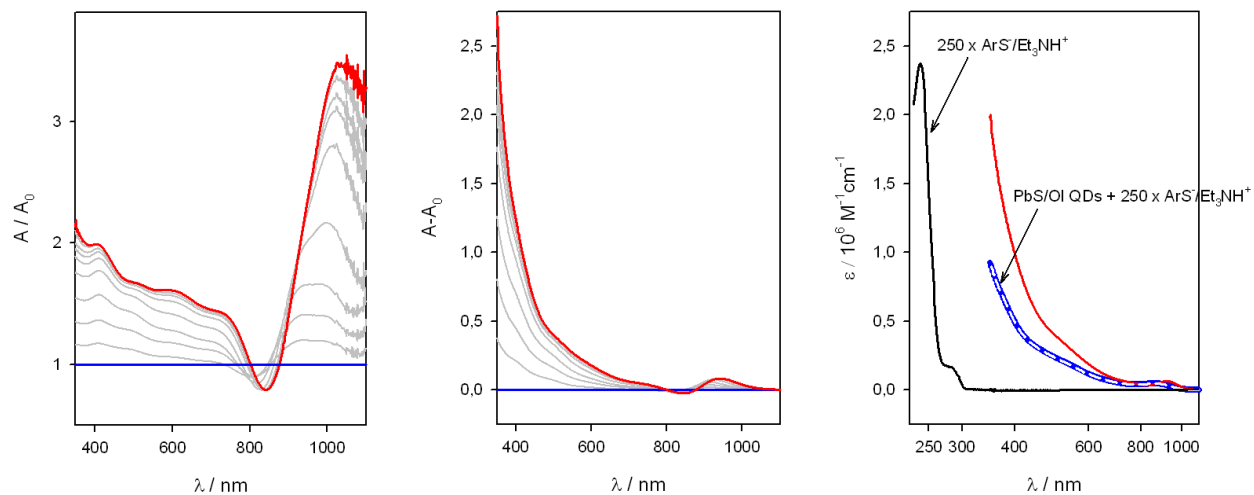


Figure S23. Ratiometric (left) and differential (centre) optical absorption spectra of a 2.5 μM dichloromethane solution of colloidal PbS/OI QDs (blue lines), upon addition of $\text{ArS}^-/\text{Et}_3\text{NH}^+$ (grey lines) up to about 750 equivalents (red lines) as reported in Figure 2a. right) Sum absorption spectrum of PbS/OI QDs + 250 equivalents of ArS^- ligands (white dashed line) coincides with PbS/OI QDs spectrum (blue line); red line represents PbS/ArS QDs.

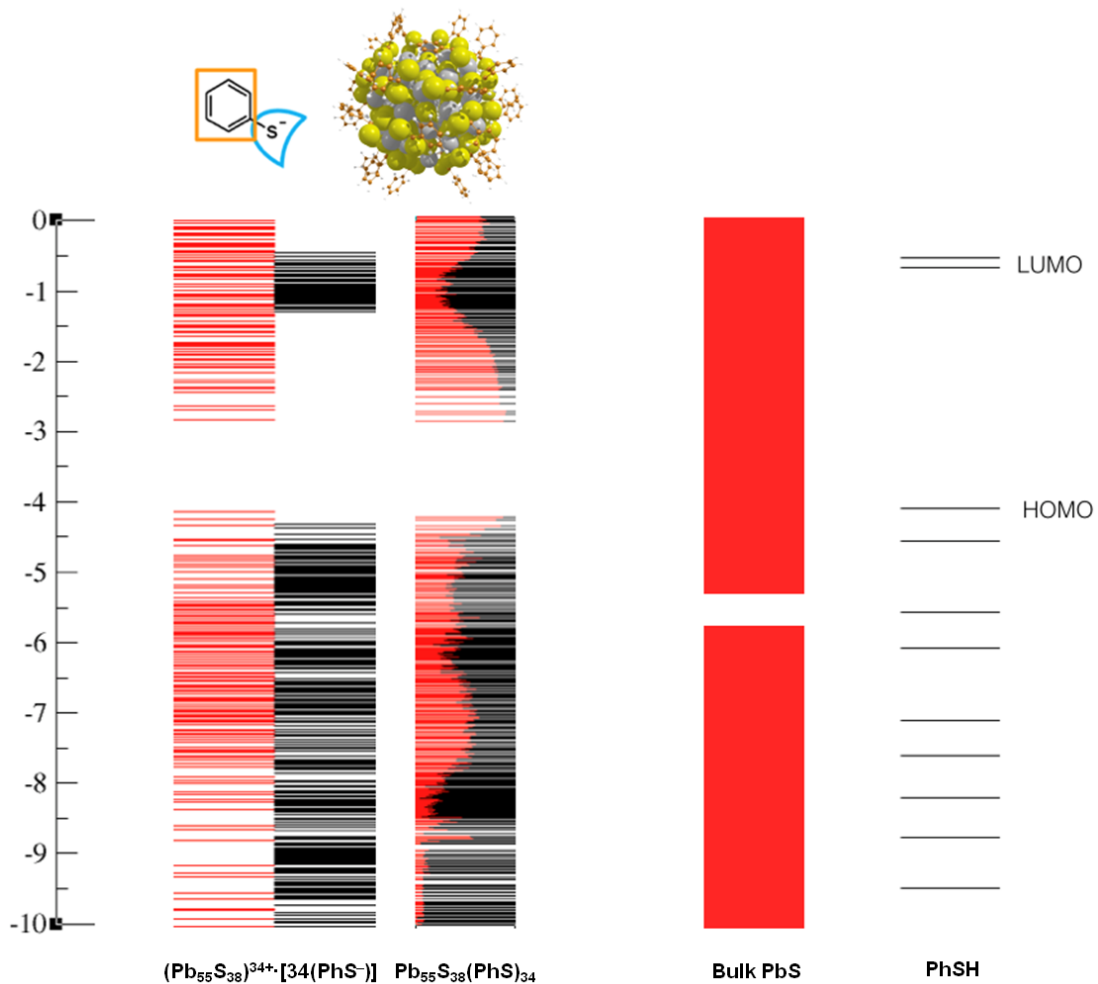


Figure S24. Calculated ligand/cluster orbitals for the model $(\text{Pb}_{55}\text{S}_{38})^{34+}$ clusters capped with 34 PhS^- ligands. Orbitals appearing with mixed red-black color are delocalized orbitals of the entire ligand/cluster system, whereas orbitals on the left side represent contribution of ligands (black) and core (red) experiencing each other's electric field. On the right side, bulk PbS band energies and calculated DOS for isolated PhSH ligands.

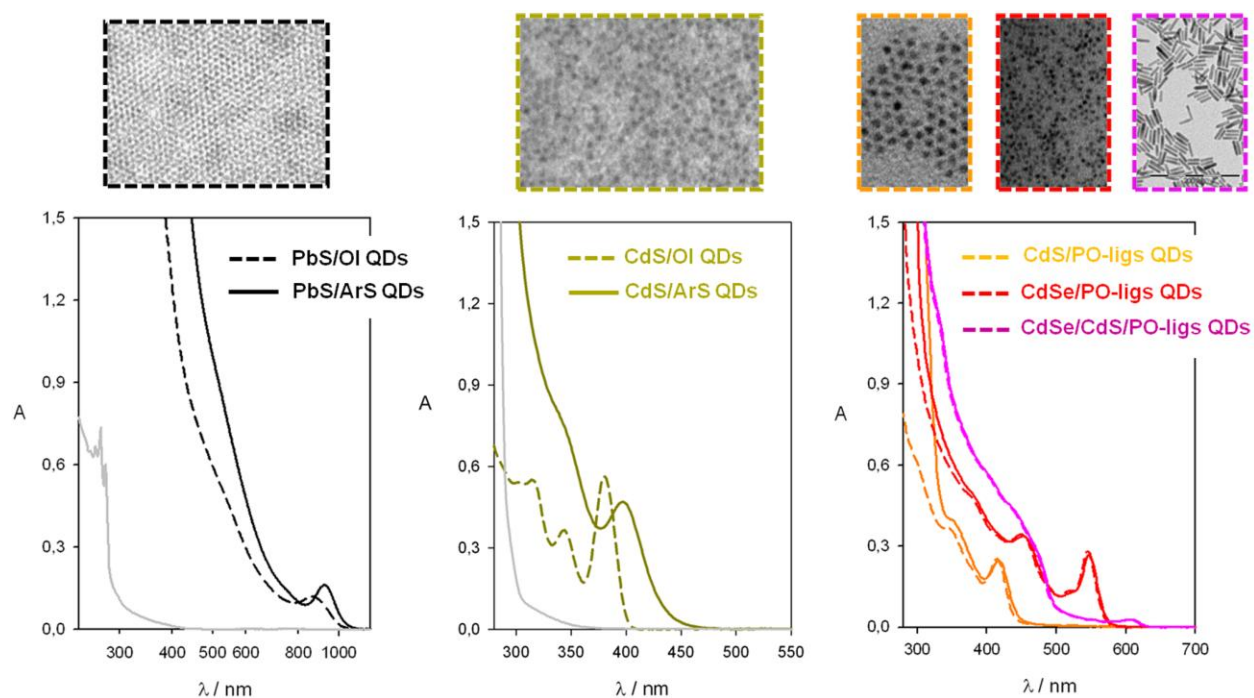


Figure S25. Left) Absorbance spectra of dichloromethane air-equilibrated solutions of colloidal PbS/OI QDs (dashed black line), PbS/ArS QDs (solid black line), and of 0.3 mM Pb(II)-oleate in dichloromethane solution upon addition of 2 equivalents of $\text{ArS}^-/\text{Et}_3\text{NH}^+$ (gray line). Center) Absorbance spectra of dichloromethane air-equilibrated solutions of colloidal CdS/OI QDs (dashed yellow line), CdS/ArS QDs (solid yellow line), and of 0.3 mM Cd(II)-oleate in dichloromethane solution upon addition of 2 equivalents of $\text{ArS}^-/\text{Et}_3\text{NH}^+$ (gray line). Right) Absorbance spectra of dichloromethane air-equilibrated solutions of colloidal CdS QDs (orange lines), CdSe QDs (red lines), and CdSe/CdS QDs (purple lines) capped with alkyl phosphine oxide and phosphonic acids (dashed lines) and upon addition of a large excess of $\text{ArS}^-/\text{Et}_3\text{NH}^+$ (solid lines). TEM images of as-synthesized QDs are shown on top of corresponding absorption spectra.

Supporting References

1. Hines, M. A.; Scholes, G. D., *Advanced Materials* **2003**, *15* (21), 1844-1849.
2. Moreels, I.; Lambert, K.; Smeets, D.; De Muynck, D.; Nollet, T.; Martins, J. C.; Vanhaecke, F.; Vantomme, A.; Delerue, C.; Allan, G.; Hens, Z., *ACS Nano* **2009**, *3* (10), 3023-3030.
3. Yu, W. W.; Peng, X., *Angewandte Chemie International Edition* **2002**, *41* (13), 2368-2371.
4. Yu, W. W.; Qu, L.; Guo, W.; Peng, X., *Chem. Mater.*, **2003**, *15* (14), 2854-2860.
5. Carbone, L.; Nobile, C.; De Giorgi, M.; Sala, F. D.; Morello, G.; Pompa, P.; Hytch, M.; Snoeck, E.; Fiore, A.; Franchini, I. R.; Nadasan, M.; Silvestre, A. F.; Chiodo, L.; Kudera, S.; Cingolani, R.; Krahne, R.; Manna, L., *Nano Letters* **2007**, *7* (10), 2942-2950.
6. Giansante, C.; Carbone, L.; Giannini, C.; Altamura, D.; Ameer, Z.; Maruccio, G.; Loiudice, A.; Belviso, M. R.; Cozzoli, P. D.; Rizzo, A.; Gigli, G., *The Journal of Physical Chemistry C* **2013**, *117* (25), 13305-13317.
7. Jasieniak, J.; Mulvaney, P., *Journal of the American Chemical Society* **2007**, *129* (10), 2841-2848.
8. Moreels, I.; Fritzing, B.; Martins, J. C.; Hens, Z., *Journal of the American Chemical Society* **2008**, *130* (45), 15081-15086.
9. Hens, Z.; Moreels, I., *Journal of Materials Chemistry* **2012**, *22* (21), 10406-10415.
10. Neeves, A. E.; Bimboim, M. H., *J. Opt. Soc. Am. B* **1989**, *6* (4), 787-796.
11. Wang, Y.; Suna, A.; Mahler, W.; Kasowski, R., *The Journal of Chemical Physics* **1987**, *87* (12), 7315-7322.
12. Hunger, J.; Stoppa, A.; Thoman, A.; Walther, M.; Buchner, R., *Chemical Physics Letters* **2009**, *471* (1-3), 85-91.
13. www.aldrich.com
14. Leatherdale, C. A.; Bawendi, M. G., *Physical Review B* **2001**, *63* (16), 165315.
15. Allan, G.; Delerue, C.; Lannoo, M.; Martin, E., *Physical Review B* **1995**, *52* (16), 11982-11988.